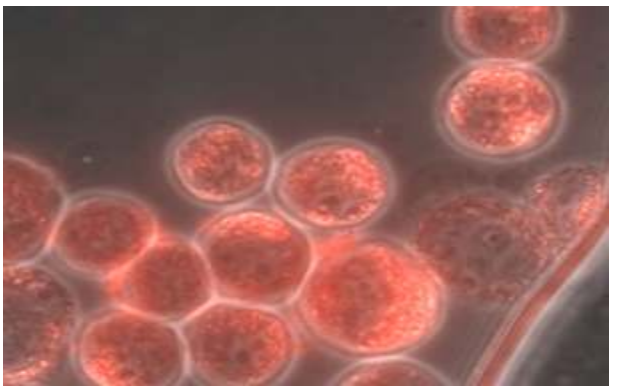

Fig. L.10.2: Fluorescence images (superimposed with phase contrast image) of Colo cells containing Nile Red doped Si-NPs after one hour incubation time. Excited at 532 nm and emission collected after 580 nm.

To use these fluorescent Si-NPs for cellular imaging, C35 is not a desirable fluorescence label because its excitation is near UV region, which may adversely affect cells. Therefore, the Si-NPs were loaded with another fluorescent dye, Nile red, having excitation wavelength in the green region and its uptake was monitored in the Colo cells by fluorescence microscopy. Incubation of Colo cells with Nile Red doped Si-NPs was observed to lead to significant intracellular staining (Fig.L.10.2). These results show that Si-NPs with appropriate functionalization may be used as fluorescent probes to target intracellular objects.

Contributed by:
K Das (kaustuv@cat.ernet.in), A. Uppal, B. Jain, B.Bose, and P. K. Gupta

L.11 : Development of high power laser diodes

High power laser diodes in the wavelength range of 740 nm to 1000 nm have been developed in the Semiconductor Laser Section of SSLD. The complete laser structure was grown by metal organic vapour phase epitaxy (MOVPE) technique. A typical semiconductor laser structure is consisted of about 10 epilayers with different composition, thickness and doping values. For example, a laser diode operating at 0.8 μm has either GaAs or GaAsP quantum well as an active layer. The quantum well is sandwiched between AlGaAs wider band gap waveguide and cladding layers. Laser structures were characterized using several techniques like photoluminescence, surface photo voltage and high resolution x-ray diffraction techniques. The ionized doping and free carrier density were estimated from Hall and ECV experiments. The net ionized doping was also estimated at different depth of the laser diode structures using ECV. Laser diodes were fabricated through standard procedure using photolithography process. A quick method of laser diode processing has also been successfully implemented using shadow mask technique. Laser diodes were tested for light versus current and longitudinal characteristics using a home-made current source. Laser diodes with different cavity lengths and widths were also developed and tested for measuring the device parameters. For the laser diodes developed, an internal quantum efficiency of 92% and internal loss of 4 cm^{-1} was measured. More than 5 watt peak power at several wavelengths was achieved.

Contributed by :
T. K. Sharma (tarun@cat.ernet.in)

L.12 : Fundamental studies on MOVPE grown semiconductor heterostructures

a. Studies on MOVPE growth of GaP epitaxial layer on Si (0 0 1) substrate and effects of annealing :

Growth of gallium phosphide layer on silicon substrate has been carried out using MOVPE. Epitaxial layers were grown at 845°C with a V/III ratio of 100 and a growth rate of 1.7Å/s at a reactor pressure of 30mbar. Growth of gallium phosphide epilayer was confirmed by Raman spectra studies. High-resolution x-ray diffraction studies show that the epilayer is of single crystalline nature and structurally coherent with silicon substrate. As-grown epilayer shows p-type behavior with a hole carrier density of ~$1.2x10^{18}cm^{-3}$ and hole mobility $114cm^2$/V-sec at room temperature. Annealing at 550°C for 10 minutes shows significant improvements in crystalline quality of the epilayer. The annealed layer shows a reduced hole density (~$6.7x10^{17}cm^{-3}$) and increased hole mobility ($155cm^2$/V-s). [*Ref: Dixit et. al., J. Crystal Growth 293, 5, 2006*]

b. Transport properties of two dimensional electron gas for $Al_{0.4}Ga_{0.6}As$ / GaAs heterojunction : Classical and Quantum Hall studies :

Studies on classical and quantum Hall-effect were carried out at Semiconductor Laser Section on two dimensional electron gas (2DEG) system of Al_xGa_{1-x} As/GaAs for critical value of x=0.4 (composition where conduction valleys cross over from Γ to X at room temperature). The structures were grown at 770°C using MOVPE technique. The exposure of light provides the persistent photoconductivity conditions, which gives sheet electron density of 1.05 x $10^{12}cm^{-2}$ with its mobility 28911.3m^2 $V^{-1}s^{-1}$ in the 2DEG system. The Hall resistance (R_{XY}) shows plateaus at high field (>3 tesla) which is the confirmation of 2DEG and quantization as h/ve^2. The filling fraction (ν) decreases as magnetic field increases confirming increase in the degeneracy. These plateaus become feeble at 18K and disappear at T > 20K. At this temperature, the thermal energy (k_BT) is comparable to the cyclotron energy (ħω) and hence modulation of density of states is not significant. As a result, quantum Hall signal disappears and the system shows classical Hall effect. The longitudinal resistance (R_{xy}) shows Shubnikov de Hass oscillations with

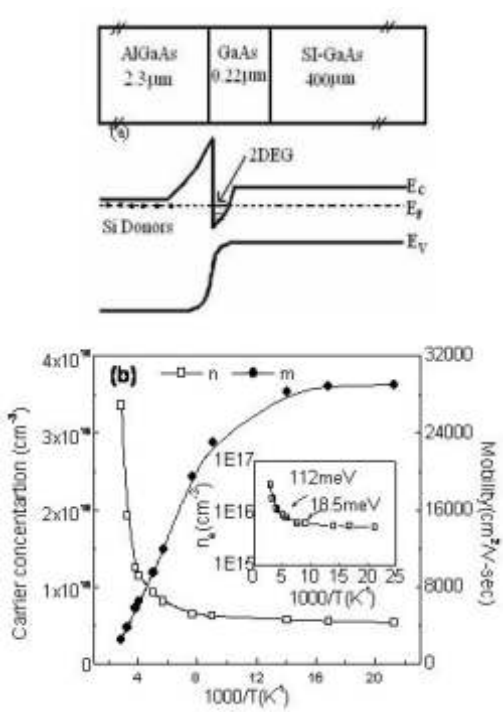

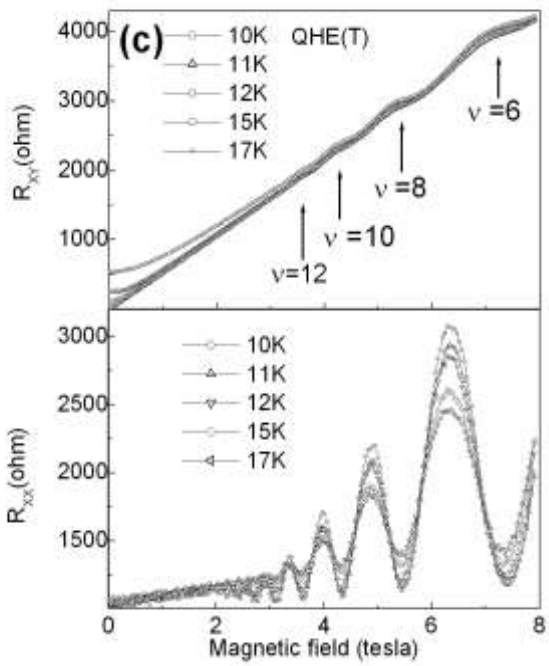

Fig.L.12 : a). Schematic of 2DEG formation in $Al_{0.4}Ga_{0.6}$ As/ GaAs heterostructure b, c). Temperature dependent low magnetic and high magnetic field transport data of $Al_{0.4}Ga_{0.6}$ As/ GaAs

increasing magnetic field. From temperature (4.2-20 K) and magnetic field (up to 8T) dependent R_{xy} and R_{xy} measurements, many parameters such as effective mass of electron ($m_e^* = 0.062m_o$) and single particle scattering time (t_s = 0.178ps) of 2DEG system (Fig.L.12) have been estimated.

c. Spectroscopic investigations of InGaAs / GaAs quantum wells with low and high built-in strain :

MOVPE grown InGaAs quantum wells (QW) with low and high built-in strain were investigated at Semiconductor Laser Section by using complementary spectroscopic techniques like photoluminescence (PL) and surface photo-voltage spectroscopy (SPS). The built-in strain was varied by increasing the indium content while keeping the QW thickness constant. It was shown that the SPS technique provides more information about strained QW samples as compared to routinely used PL technique. It could be used even when there is no PL signal detected from a

highly strained QW sample due to either presence of high defect/dislocation density or thermal escape of charge carriers the in case of a shallow QW. The indium content of 0.42 represents an onset for the 2D-3D growth transition for the InGaAs QWs grown under present conditions, which was supported by low-temperature PL, room-temperature SPS and HRXRD data. Various transitions seen in the SPS spectra were identified by solving the Schrödinger equation for one dimensional square potential well. [*Ref: T.K.Sharma et. al., J. Crystal Growth 298, 527, 2007*]

Contributed by :
V. K. Dixit (dixit@cat.ernet.in) and
T. K. Sharma (tarun@cat.ernet.in)

L.13 : Studies on GaN and GaP nanostructures :

a. GaN nanostructures : A detailed study was carried out on nanotextured high density Mg-doped GaN and undoped GaN, using photoluminescence spectroscopy. Nanotextured high-density Mg-doped and undoped GaN were obtained using photo-electrochemical etching. Fig.L.13.1: SEM image of a nanotextured GaN. Interesting features are observed in the temperature dependent photo-luminescence (PL) studies of these nanotextured materials. First, the PL intensity of the excitonic emissions shows more than three orders of magnitude enhancement. At low temperature, the peak energy shows a blue-shift with temperature. Second, the excitonic emissions in the nanotextured samples are red-shifted compared to the as-grown GaN suggesting strain relaxation. Third, the blue luminescence band (2.7 - 2.9 eV in Mg-doped GaN) shows a large red-shift, which is not consistent with strain relaxation calculated from excitonic band Furthermore, temperature dependence of the blue luminescence band energy shows an asymmetric S-shaped behavior in nanotextured GaN. All these observations are explained by invoking increase in carrier localization due to increase in potential fluctuation created by the nanotexturization process. [*Ref: S.Pal. et. al., J.Appl. Phys. 101, 044311, 2007*]

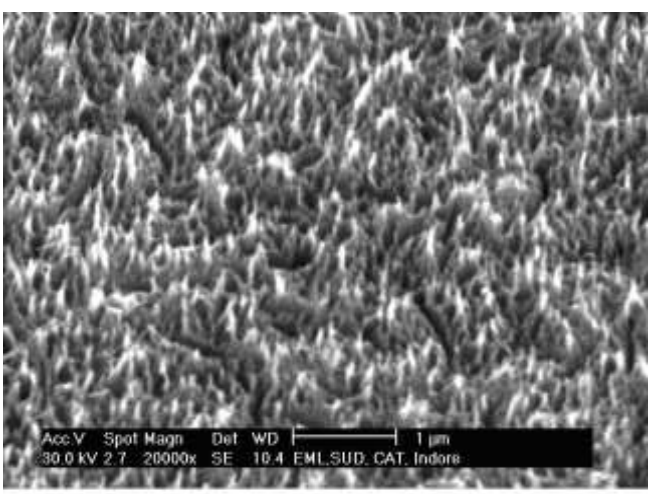

Fig.L.13.1: SEM image of a nanotextured GaN

b. GaP nanostructures : Detailed studies were carried out on GaP wafer and nanoporous GaP network samples, using photoluminescence (PL) spectroscopy. SEM photograph of nanoporous GaP shown in Fig L. 13.2. Pore size is 140 ± 30nm with 44% porosity and the effective refractive index of these structure is ~ 1.50 ± 0.1. The PL signal is largely enhanced for band to band transition and a new luminescence is observed in visible and deep blue spectral range. The valence bands offset between porous GaP and GaO_x is found to be 2.30eV at room temperature. [*Ref: V.K.Dixit et al. Appl. Phys. Lett., 88, 083115, 2006*]

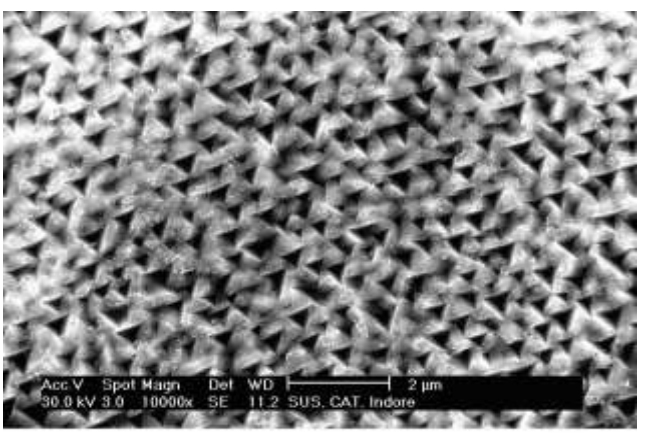

Fig.L.13.2: SEM photograph of nanoporous GaP

Contributed by :
Suparna Pal (suparna@cat.ernet.in) and
V. K. Dixit (dixit@cat.ernet.in)